Competitive Reactions of Atomic Oxygen with Acetone on Ag(110): Nucleophilicity Versus Basicity

Caroline R. Ayre[†] and Robert J. Madix*[,‡]

Contribution from the Departments of Chemistry and Chemical Engineering, Stanford University, Stanford, California 94305-5025

Received May 18, 1994[⊗]

Abstract: Acetone (2-propanone, $(CH_3)_2CO$) exposed to oxygen-activated Ag(110) at 110 K reacts via *both* nucleophilic attack of oxygen at the electron-deficient carbonyl carbon and C−H bond activation. The former process results in the reversible formation of the metallacycle $(CH_3)_2COO_{(a)}$, an outcome indicated by the incorporation of $^{18}O_{(a)}$ into all products evolving at ≥215 K during temperature-programmed reaction spectroscopy experiments in which ^{18}O atoms are preadsorbed. This facile exchange of surface oxygen atoms with $(CH_3)_2COO_{(a)}$ indicates that this reversible transfer is a general type of reaction on Ag(110). Cleavage of a C−O bond in $(CH_3)_2COO_{(a)}$ occurs at 215 and 330 K to liberate acetone from the surface. C−H bond activation by $O_{(a)}$ yields acetone enolate (CH_2=C-$(CH_3)O_{(a)}$) and results in both the evolution of $H_2O_{(g)}$ at 220 K and the disproportionation of hydroxyl groups ($OH_{(a)}$) to yield additional $H_2O_{(g)}$ at 300−330 K. The activation of the C−H bond is predicted from the gas-phase acidity of acetone. Acetone is re-formed by enolate disproportionation at 445 K, but no acetone enol is detected in the gas phase. Partial oxidation of adsorbed species yields $CO_{2(g)}$ at 405 and 475 K, $H_2O_{(g)}$ at 450 K, and residual adsorbed hydrocarbon fragments.

1. Introduction

Acetone (2-propanone), the simplest ketone, possesses two chemically different sites for potential activation by adsorbed atomic oxygen on silver(110): (1) an electron-deficient acyl carbon and (2) six equivalent acidic methyl C−H bonds. As a result, acetone is an excellent candidate for study in order to compare the relative importance of nucleophilicity and basicity in bond activation by atomic oxygen. In addition, the reactivity of acetone on this surface may be compared with that of a number of other carbonyl compounds whose interactions with oxygen-activated Ag(110) have been investigated, including formaldehyde,[1,2] formic acid,[2,3] acetaldehyde,[4] acetic acid,[4] and methyl formate.[1] Formic acid (HCOOH) and acetic acid (CH_3-COOH), for example, react stoichiometrically with $O_{(a)}$ on Ag(110) to form adsorbed formate ($HCOO_{(a)}$) and acetate (CH_3-$COO_{(a)}$), respectively. However, adsorbed atomic oxygen reacts via nucleophilic attack at the carbonyl carbon of formaldehyde (H_2CO), acetaldehyde (CH_3CHO), and methyl formate (HCO-OCH_3) to yield the corresponding adsorbed carboxylates, and, for $HCOOCH_3$, the methoxide ($OCH_{3(a)}$).[1,2,4] In this study, the interaction of acetone with oxygen-activated Ag(110) has been explored using temperature-programmed desorption (TPD), temperature-programmed reaction spectroscopy (TPRS), isotopic labeling, surface titration experiments, and electron energy loss vibrational spectroscopy (EELS).

2. Experimental Section

Experiments were performed in two different stainless steel vacuum chambers with base pressures of ≈2 × 10^{-10} Torr. The two chambers are described in detail elsewhere.[5,6] Two different Ag(110) crystals were employed. Each crystal was held in a tantalum foil mount spot-welded to tantalum support wires. Both crystals were cooled to *ca.* 110 K by thermal conduction via support rods connected to a copper block containing a liquid nitrogen reservoir. The crystal used in TPRS experiments was heated radiatively by a tungsten filament suspended 1−3 mm behind the mount. The crystal used in the EELS experiments was heated resistively. Heating rates of ≈6 K s^{-1} were achieved by both methods.

Clean Ag(110) surfaces were prepared by argon ion bombardment (400−500 eV; 6−8 μA cm^{-2}) at 300 K, followed by an 800 K anneal to restore surface long-range order. Sample cleanliness was verified by a combination of Auger electron spectroscopy (AES) and temperature-programmed desorption (TPD). Oxygen titration of carbon impurities was then carried out until the residual $CO_{2(g)}$ desorption yield in a TPD experiment was less than 3% of the $O_{2(g)}$ yield for a given oxygen exposure. Adsorbed oxygen coverages were calculated by comparing the $O_{2(g)}$ yield for a particular oxygen exposure with that obtained for a saturation exposure, previously determined to be 0.50 monolayer (ML) of $O_{(a)}$ on Ag(110).[7]

Temperature-programmed reaction data were collected using a UTI 100C mass spectrometer interfaced to a PDP 11/03 DEC computer. A glass cap with an aperture approximately 3 mm in diameter was attached to the mass spectrometer ionization cage to collimate the flux desorbing from the crystal surface, which was positioned 1−2 mm in front of the opening. Initial experiments were conducted using a program which allowed a maximum of 200 ions to be monitored for product identification.[8] Subsequent spectra were recorded by monitoring no more than eight ions simultaneously during a 20-ms scan for improved temperature resolution. All TPD/TPR spectra have been corrected for mass spectrometer ionization efficiency, gain, and transmission using the method of Ko *et al.*[9]

EEL spectra were recorded in the specular direction using an LK2000 high resolution electron energy loss spectrometer.[10] Typical resolution of the elastic peak from adsorbate-covered Ag(110) was 56−64 cm^{-1} with a count rate of approximately 1.5 × 10^4 − 3 × 10^5 Hz for a beam energy of ≈5 eV. All spectra were recorded at a crystal temperature of 110 K after annealing the sample to the temperatures indicated below.

[†] Department of Chemistry. Current address: Intel Corporation, 2200 Mission College Blvd., SC2-24, Santa Clara, CA 95052-8119.
[‡] Department of Chemical Engineering.
[⊗] Abstract published in *Advance ACS Abstracts,* January 1, 1995.
(1) Barteau, M. A.; Bowker, M.; Madix, R. J. *Surf. Sci.* **1980**, *94*, 303.
(2) Stuve, E. M.; Madix, R. J.; Sexton, B. A. *Surf. Sci.* **1982**, *119*, 279.
(3) Sexton, B. A.; Madix, R. J. *Surf. Sci.* **1981**, *105*, 177.
(4) Barteau, M. A.; Bowker, M.; Madix, R. J. *J. Catal.* **1981**, *67*, 118.
(5) Madix, R. J. *Surf. Sci.* **1979**, *89*, 540.
(6) Ayre, C. R. PhD. Dissertation, Stanford University, 1992.
(7) Englehardt, H. A.; Menzel, R. *Surf. Sci.* **1976**, *57*, 591.
(8) Capote, A. J.; Madix, R. J. *Surf. Sci.* **1989**, *214*, 276.
(9) Ko, E. I.; Benziger, J. B.; Madix, R. J. *J. Catal.* **1980**, *62*, 264.
(10) Kesmodel, L. L. *J. Vac. Sci. Technol. A* **1983**, *1*, 1456.

0002-7863/95/1517-2301$09.00/0

Table 1. Experimentally-Determined Enhancement Factors for Reagents[a]

apparatus	chemical name	enhancement factor
TPRS chamber	oxygen/oxygen-18	100[b]
	acetone	60
	formic acid-*O*-*d*	100[b]
EELS chamber	oxygen	26
	acetone/acetone-d_6	60

[a] In all cases, oxygen and hydrocarbons were introduced through separate dosing valves to avoid cross-contamination. A capillary dosing array was used unless otherwise indicated. [b] Stainless steel needle valve.

For both EELS and TPRS experiments, all acetone exposures were made with the Ag(110) surface temperature held at 110 K. Furthermore, TPRS experiments were repeated in the EELS chamber in order to confirm that TPRS data were reproducible. EELS data were collected on an X−Y recorder and the resultant spectra digitized by hand to produce the figures shown here.

Acetone-d_0 ($(CH_3)_2CO$: Baker, 99.4%) was dried with potassium carbonate (K_2CO_3) overnight, as recommended by Perrin and coworkers, prior to vacuum transfer to an oven-dried sample tube.[11] Because acetone-d_6 is highly hygroscopic, this compound ($(CD_3)_2CO$: Aldrich, 99.96 atom % D) was transferred in a nitrogen atmosphere (drybox) to a flask, dried with K_2CO_3 overnight, and then transferred, again under nitrogen, to an oven-dried sample tube. Both $(CH_3)_2CO$ and $(CD_3)_2CO$ were further purified with freeze−pump−thaw cycles daily prior to use. The absence of H_2O in each sample was verified each day prior to conducting experiments by exposing a clean Ag(110) surface to $(CH_3)_2CO_{(g)}$ or $(CD_3)_2CO_{(g)}$, as appropriate, and monitoring for $H_2O_{(g)}$ desorption by temperature-programmed desorption (TPD). Formic acid-*O*-*d* (HCOOD): (Cambridge Isotope Labs, 95% in 5% D_2O) was degassed by freeze−pump−thaw cycles as well. Oxygen (Matheson, 99.6 %), oxygen-18 (ICN Biomedical, 99.0%), acetylene-d_2 (Cambridge Isotope Labs, 99.0 atom % D), and carbon monoxide (Matheson, 99.5%) were used as received. The purities of all compounds were verified *in situ* by mass spectrometry.

All exposures are reported in langmuirs (1 L = 10^{-6} Torr·s) and are corrected for the flux enhancement provided by directed dosing. Measured enhancement factors appear in Table 1. The enhancement factor is defined as the ratio of the area of the TPD peak for a reactant exposure with the crystal facing the doser (direct dose) to the area of the TPD peak for an exposure of equal pressure and duration for the same gas with the crystal facing away (background dose). An exposure is defined as the product of the background chamber pressure (from uncorrected nude ion gauge readings), the duration of the exposure (in seconds), and the appropriate enhancement factor for the gas of interest.

3. Results and Discussion

A. Temperature-Programmed Reaction Spectroscopy (TPRS). (a) Reaction with Atomic Oxygen ($^{16}O_{(a)}$). Preadsorbed atomic oxygen reacts with acetone on Ag(110) via *both* C−H bond activation and nucleophilic attack. Temperature-programmed reaction spectra obtained following the exposure of a Ag(110) surface covered with a 0.25 ML of $O_{(a)}$ to 3 L of $(CH_3)_2CO_{(g)}$ appear in Figure 1. The reactivity of the Ag(110) surface toward acetone in the presence of adsorbed atomic oxygen is clearly indicated by the evolution of three acetone states at temperatures of 215 (shoulder), 330, and 445 K in TPRS, which are not observed on the clean surface (dotted spectrum in Figure 1). In addition, $H_2O_{(g)}$ is produced at 220, 300, 330, and 450 K, and $CO_{2(g)}$ evolves at 405 and 475 K. No additional products evolve. An extensive search for evidence of the evolution of the enol tautomer of acetone, acetone enol (2-hydroxypropene, $CH_3C(OH)=CH_{2(g)}$), in particular, was carried out because vibrational spectra indicate the presence of acetone enolate ($CH_2=C(CH_3)O_{(a)}$) (discussed below). Based on the mass spectra of the acetone radical cation $[CH_3C(O)CH_3]^{+\cdot}$ and the acetone enol radical cation $[(CH_3C(OH)=CH_2]^{+\cdot}$ reported by Turecek and Hanus for ionizing electrons of 75 eV kinetic energy, detection of acetone enol as a product in TPRS should have been possible here.[12] Although the fragmentation patterns of the two species are similar, higher abundances (relative to *m/q* 43 = 100% fragment for both species) of the following fragments of acetone enol, as compared with those of acetone, have been reported by these authors (Table 2): *m/q* 58 (molecular ion), *m/q* 57 $(C_3H_5O)^+$, *m/q* 39 $(C_3H_3)^+$, *m/q* 31 $(CH_3O)^+$, and *m/q* 29 $[(CHO)^+ + (C_2H_5)^+]$. Furthermore, the stability of the acetone enol (molecular) radical cation has been reported to be greater than that of the keto form, whereas the neutral keto form is more stable in the gas phase.[13,14] In TPRS experiments, however, the fragmentation pattern relative to *m/q* 43 for each product state with *m/q* 58 as the parent ion was identical with the pattern obtained for acetone desorbing from

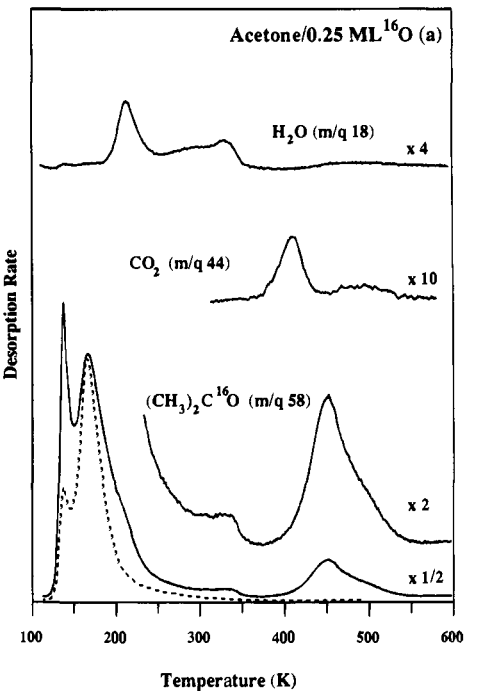

Figure 1. Temperature-programmed reaction spectra of acetone (*m/q* 58), carbon dioxide (*m/q* 44), and water (*m/q* 18) produced from the reaction of 3 L of acetone with 0.25 ML of $O_{(a)}$ on Ag(110). Heating rate (β) $\approx$ 6 K s^{-1}. Corrections for the fragmentation of acetone have been subtracted from the *m/q* 44 and *m/q* 18 spectra. The temperature-programmed desorption (TPD) spectrum for acetone (*m/q* 58) evolving without reaction from clean Ag(110) (dotted line) following a 1 L $(CH_3)_2CO$ exposure is provided for comparison.

Table 2. Selected Mass Spectral Fragments of Acetone and Acetone Enol[a]

mass-to-charge ratio (*m/q*)	fragment(s)	relative abundances (%) $(CH_3)_2CO$	relative abundances (%) $CH_2=C(OH)CH_3$
58	$[CH_2=C(OH)CH_3]^{+\cdot}$ $[CH_3C(O)CH_3]^{+\cdot}$	20	47
57	$[C_3H_5O]^+$	1.1	7.7
43	$[C_2H_3O]^+$	100	100
39	$[C_3H_3]^+$	5.5	14
31	$[CH_3O]^+$	0.7	12
29	$[CHO]^+$ $[C_2H_5]^+$	2.9	22

[a] From ref 12.

(11) Perrin, D. D.; Amarego, W. L. F.; Perrin, D. R. *Purification of Laboratory Chemicals*; Pergamon Press: Oxford, 1980; p 79.

(12) Turecek, F.; Hanus, V. *Org. Mass Spectrom.* **1984**, *19*, 631.
(13) Holmes, J. L.; Lossing, F. P. *J. Am. Chem. Soc.* **1980**, *102*, 1591.
(14) Chiang, Y.; Kresge, A. J.; Schepp, N. P. *J. Am. Chem. Soc.* **1989**, *111*, 3977.

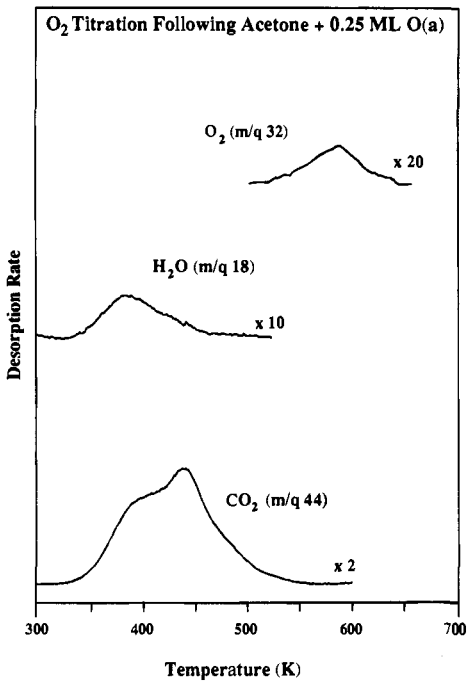

Figure 2. Temperature-programmed reaction spectra of cleanoff of residual hydrocarbons following TPRS experiment described in Figure 1. O_2 exposure (at 300 K) was sufficient to have produced 0.30 ML of $O_{(a)}$ on clean Ag(110). Heating rate $\beta \approx 6$ K s^{-1}.

clean Ag(110). This result clearly indicates that the enol tautomer was not detected.

The evolution of molecularly-bound H_2O at the characteristic desorption temperature of 220 K clearly indicates that scission of one or more C−H bonds in acetone occurs below this temperature. Evolution of $H_2O_{(g)}$ due to $OH_{(a)}$ disproportionation from 300−330 K provides further evidence of C−H bond activation by adsorbed oxygen. The production of $CO_{2(g)}$ and $H_2O_{(g)}$ at higher temperatures is indicative of the combustion of acetone-derived intermediates by scavenging $O_{(a)}$ atoms released during $OH_{(a)}$ disproportionation. Hydrocarbon fragments produced by the incomplete reaction of $(CH_3)_2CO_{(a)}$ remain adsorbed on the surface following a TPRS experiment. Exposure of the surface at 300 K to $O_{2(g)}$ following an acetone TPRS experiment yields both $CO_{2(g)}$ and $H_2O_{(g)}$ upon heating (Figure 2). The yield of $CO_{2(g)}$ in the cleanoff experiment (Figure 2) relative to the amount of carbon dioxide produced during an acetone TPRS experiment (Figure 1) is $\approx 23 : 1.0$. The surface was clean following a single oxygen titration experiment.

(b) Isotopic Labeling Experiments. When oxygen-18 atoms are pre-adsorbed on Ag(110), they exchange with the oxygen-16 atoms of the 215 K $(CH_3)_2C^{16}O$ state to yield comparable amounts of $(CH_3)_2C^{18}O_{(g)}$ and $(CH_3)_2C^{16}O_{(g)}$ simultaneously at 215 K (Figure 3). No ^{18}O exchange with the 170 K molecular state is observed. With heating, both $(CH_3)_2C^{16}O$ and $(CH_3)_2C^{18}O$ evolve at 330 and 445 K. Both water isotopes $H_2{}^{18}O$ and $H_2{}^{16}O$, as well as the three carbon dioxide isotopes $C^{18}O_2$, $C^{18}O^{16}O_2$, and $C^{16}O_2$, are produced at the temperatures reported above (Figure 4). These results strongly suggest that adsorbed acetone reacts to produce the bidentate metallacycle $(CH_3)_2C^{18}O^{16}O_{(a)}$ *below* 215 K:

$$(CH_3)_2C^{16}O_{(a)} + {}^{18}O_{(a)} \rightarrow (CH_3)_2C^{16}O^{18}O_{(a)} \qquad (1)$$

which reversibly yields acetone when heated. Hence, the statistical probability of producing $(CH_3)_2C^{18}O_{(a)}$ or $(CH_3)_2C^{16}O_{(a)}$ from bidentate $(CH_3)_2C^{18}O^{16}O_{(a)}$ via cleavage of either carbon−oxygen bond in the reverse reaction is equal:

$$(CH_3)_2C^{16}O^{18}O_{(a)} \rightarrow (CH_3)_2C^{18}O_{(g)} + {}^{16}O_{(a)} \qquad (2)$$

or

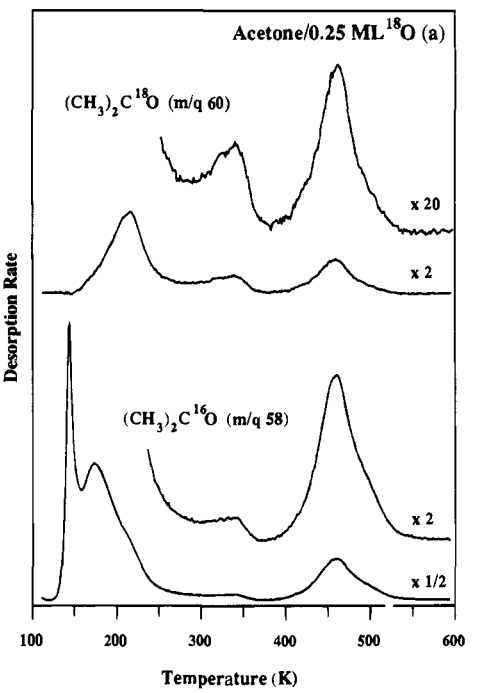

Figure 3. Evolution of $(CH_3)_2C^{16}O_{(g)}$ (*m/q* 58) and $(CD_3)_2C^{18}O_{(g)}$ (*m/q* 60) produced from the reaction of 3 L of $(CH_3)_2C^{16}O_{(g)}$ with 0.25 ML of $^{18}O_{(a)}$. The $(CH_3)_2C^{16}O$ (*m/q* 58) spectrum has been corrected for both the presence of co-adsorbed $^{16}O_{(a)}$ and the fragmentation of *m/q* 60. Heating rate $(\beta) \approx 6$ K s^{-1}.

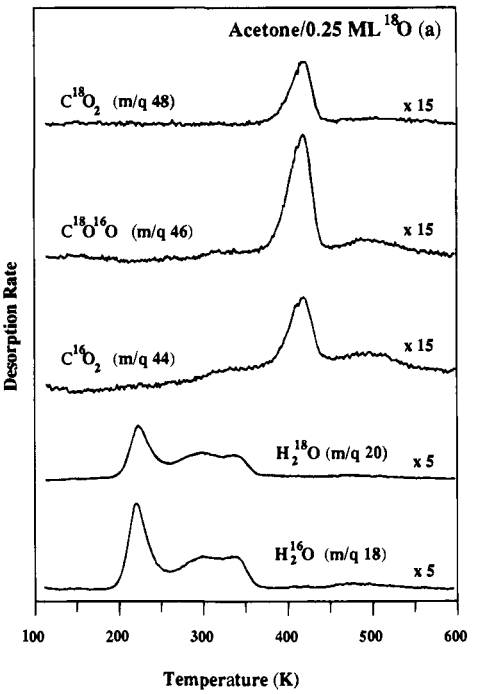

Figure 4. Evolution of water and carbon dioxide isotopes produced from the reaction of 3 L of $(CH_3)_2C^{16}O_{(g)}$ with 0.25 ML $^{18}O_{(a)}$. The $C^{16}O_{2(g)}$ (*m/q* 44) and $C^{18}O^{16}O_{(g)}$ (*m/q* 46) spectra have been corrected for the fragmentation of $(CH_3)_2C^{16}O_{(g)}$ (*m/q* 58) and $(CH_3)_2C^{18}O_{(g)}$ (*m/q* 60) (Figure 3). No correction of the $C^{18}O_{2(g)}$ (*m/q* 48), $H_2{}^{16}O_{(g)}$ (*m/q* 18), and $H_2{}^{18}O_{(g)}$ (*m/q* 20) spectra was required. Heating rate $(\beta) \approx 6$ K s^{-1}.

$$(CH_3)_2C^{16}O^{18}O_{(a)} \rightarrow (CH_3)_2C^{16}O_{(g)} + {}^{18}O_{(a)} \quad (3)$$

Quantitative deconvolution of the 330 K $(CH_3)_2C^{18}O_{(g)}$ and $(CH_3)_2C^{16}O_{(g)}$ peak areas supports the hypothesis that acetone is produced from the bidentate intermediate $(CH_3)_2C^{18}O^{16}O_{(a)}$ via reactions 2 and 3 at this temperature. Two corrections were subtracted from the $(CH_3)_2C^{16}O_{(g)}$ (*m/q* 58) peak (1) a correction for the presence of pre-adsorbed $^{16}O_{(a)}$ (*ca.* 8−11% of *all* pre-adsorbed atomic oxygen) and (2) a factor arising from the loss of two hydrogens from *m/q* 60 due to its fragmentation in the mass spectrometer to yield *m/q* 58 (ca. 3% of *m/q* 60 signal). Neither correction was required for the $(CH_3)_2C^{18}O_{(g)}$ (*m/q* 60) peak area. The resultant ratio of *m/q* 60: *m/q* 58 $\approx 1.1 \pm 0.3$ suggests that this state arises from decomposition of $(CH_3)_2C^{18}O^{16}O_{(a)}$, in agreement with vibrational spectra presented below.

The ratio of labeled to unlabeled acetone at 445 K (*m/q* 60: *m/q* 58 ratio $\approx 0.21 \pm 0.04$) is also consistent with a *reversible* exchange of oxygen atoms occurring between molecularly adsorbed acetone and pre-adsorbed $^{18}O_{(a)}$ at low temperature. Some adsorbed $(CH_3)_2C^{18}O_{(a)}$ produced via reactions 1 and 2 then undergoes subsequent C−H bond cleavage to form the intermediate which eventually leads to $(CH_3)_2C^{18}O_{(g)}$ evolution at 445 K. The reaction of a small amount of $(CH_3)_2C^{18}O^{16}O_{(a)}$ to yield a mixture of acetone enolate intermediates, $CH_2{=}C(CH_3)^{18}O_{(a)}$ and $CH_2{=}C(CH_3)^{16}O_{(a)}$, and hydroxyl groups, $^{16}OH_{(a)}$ and $^{18}OH_{(a)}$, is also possible, but cannot be the sole reaction pathway because a *m/q* 58:*m/q* 60 TPRS peak ratio of *ca.* 1 : 1 would then be expected at 445 K. Rather, the intermediate that evolves acetone at 445 K must be primarily the result of the reaction of acetone initially with preadsorbed oxygen.

Similar isotopic mixing has been observed when formaldehyde ($H_2CO_{(g)}$) and acetaldehyde ($CH_3CHO_{(g)}$) are exposed to oxygen-activated Ag(110) at low temperature.[1,4] In the former instance, η^2-methylenedioxy ($H_2COO_{(a)}$), an intermediate structurally similar to $(CH_3)_2COO_{(a)}$, is produced at 160 K and remains stable on the surface to near 240 K, at which temperature it decomposes to yield dihydrogen ($H_{2(g)}$) and formate ($HCOO_{(a)}$).[1] The bonding of $H_2COO_{(a)}$ through the two oxygen atoms to Ag(110) in a bidentate configuration has been confirmed by EELS.[2] Formate decomposes to produce $CO_{2(g)}$ and $H_{2(g)}$ at 410 K. Experiments in which oxygen-18 atoms were pre-adsorbed on Ag(110) prior to exposure to formaldehyde resulted in the evolution of a mixture of $H_2C^{18}O_{(g)}$ and $H_2C^{16}O_{(g)}$ molecular states at both 225 and 232 K, as well as both $C^{16}O_{2(g)}$ and $C^{16}O^{18}O_{(g)}$ due to formate decomposition at 410 K. Adsorption of $CH_3CHO_{(g)}$ on an oxygen-covered Ag(110) surface at 160 K yields the bidentate intermediate $CH_3CHOO_{(a)}$, which decomposes to $H_{2(g)}$ and acetate $CH_3COO_{(a)}$.[4] When $^{18}O_{(a)}$ atoms were pre-adsorbed, a combination of $CH_3CH^{18}O_{(g)}$ and $CH_3CH^{16}O_{(g)}$ evolved at 215 and 233 K, as did an isotopic mixture of $CH_3C^{16}O_{2(a)}$ and $CH_3CH^{18}O^{16}O$ decomposition products at 640 K. Thus, the facile exchange of oxygen atoms between co-adsorbed $(CH_3)_2COO_{(a)}$ and $^{18}O_{(a)}$ shows that reversible exchange between bidentate intermediates adsorbed on Ag(110) through two oxygen atoms and co-adsorbed atomic oxygen is a general type of reaction on this surface.

(c) Surface Titration (Displacement) Experiments. In order to determine how many C−H bonds are broken in the initial attack by oxygen atoms on acetone, surface displacement reactions were conducted in which attempts were made to titrate the intermediate resulting in the production of acetone at 445 K from the surface with formic acid-*O*-*d* (HCOOD).[15] A

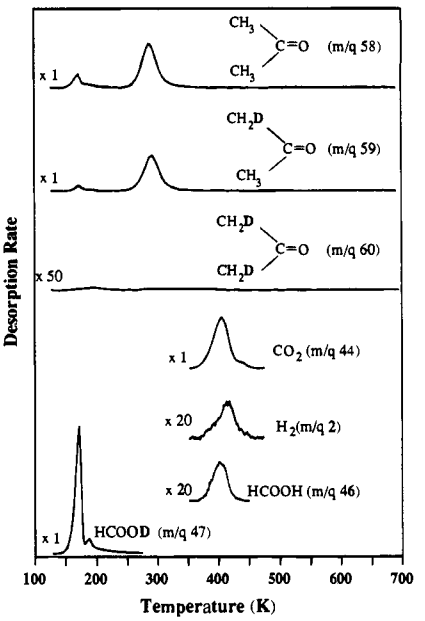

Figure 5. Products resulting from the titration of acetone enolate $CH_2{=}C(CH_3)O_{(a)}$ from Ag(110) with $HCOOD_{(g)}$. See text for explanation.

stronger gas-phase acid than acetone ($\Delta H°_{acid}$(acetone) = 369.1 ± 2.6 kcal mol^{-1}; 371.4 ± 3.5 kcal mol^{-1}),[16,17] formic acid ($\Delta H°_{acid}$(HCOOD) = 345.2 ± 2.3 kcal mol^{-1})[18] is expected to displace the adsorbed conjugate base(s) derived from the deprotonation of acetone via the mechanism:[15]

$$I_{(a)} + nHCOOD_{(a)} \rightarrow ID_{n(g)} + nHCOO_{(a)} \quad (4)$$

where I = intermediate produced from acetone and n = number of hydrogens lost by acetone to form intermediate I.

Titration of the intermediate giving rise to acetone at 445 K with HCOOD was accomplished as follows. Ag(110) activated with 0.25 ML of $O_{(a)}$ was held at 110 K and exposed to multilayers (≈3 L) of $(CH_3)_2CO$. The surface was then annealed to 420 K in order to isolate the intermediate of interest and cooled to approximately 120 K before exposure to ≈1 langmuir of HCOOD. A TPRS experiment was conducted and the evolution of product species followed by monitoring the mass-to-charge (*m/q*) ratios of acetone-d_0 through acetone-d_6 (*m/q* 58−64, inclusive). As shown in Figure 5, only acetone-d_1 (*m/q* 59) and acetone-d_0 (*m/q* 58) were evolved. $CO_{2(g)}$, $H_{2(g)}$, and $HCOOH_{(g)}$ production at 410 K is due to the decomposition of formate produced during the titration.

The evolution of *m/q* 59 at 293 K indicates that only one carbon−hydrogen bond has been broken and that the empirical formula of the intermediate giving rise to the 445 K acetone product is $CH_3C(O)CH_{2(a)}$. The *overall* reaction to produce this species is:

$$\leq 290\ K:\ CH_3C(O)CH_{2_{(a)}} + HCOOD_{(g)} \rightarrow CH_3C(O)CH_2D_{(g)} + HCOO_{(a)} \quad (5)$$

Cleavage of both equivalent methyl C−H bonds to yield $(CH_2)_2CO_{(a)}$ as a possible intermediate is unlikely because of the

(15) Barteau, M. A.; Madix, R. J. *Surf. Sci.* **1982**, *120*, 262.

(16) Bartmess, J. E.; Scott, J. A.; McIver, R. T., Jr. *J. Am. Chem. Soc.* **1979**, *101*, 6047; value reanchored in accordance with recommendation of Bartmess, J. E. "The 1987 Gas Phase Acidity Scale" (private communication).

(17) Ellison, G. B.; Engleking, P. C.; Lineberger, W. C. *J. Phys. Chem.* **1982**, *86*, 4873.

(18) Cumming, J. B.; Kebarle, P. *Can. J. Chem.* **1978**, *56*, 1.

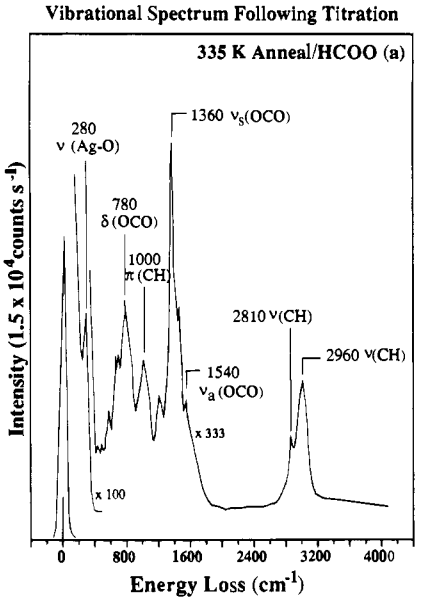

Figure 6. Vibrational spectra of formate ($HCOO_{(a)}$) and hydrocarbon fragments obtained following the evolution of acetone isotopes in the titration experiment shown in Figure 5. The surface was annealed to 335 K to desorb the acetone products and then cooled to 110 K prior to recording the spectrum on an X−Y recorder. The resultant spectrum was digitized by hand.

absence of *m/q* 60 (acetone-d_2) in TPRS. If scission of *both* acidic methyl C−H bonds had occurred to produce $(CH_2)_2CO_{(a)}$, then some amount of acetone-d_2 (*m/q* 60) product should have evolved, unless complete rehydrogenation of this intermediate is impossible. The latter is unlikely in view of the results obtained for the titration of trimethylenemethane ($(CH_2)_3C_{(a)}$) from Ag(110) with HCOOD. This intermediate, a product of the reaction of isobutylene with atomic oxygen on this surface, reacts with HCOOD to yield isobutylene-d_2 under experimental conditions identical with those used here.[6] The production of acetone-d_0 at 290 K is attributed primarily to a disproportionation reaction in which two adsorbed acetone enolate molecules combine to liberate $(CH_3)_2CO_{(g)}$ and produce adsorbed hydrocarbon fragments.

$$290\ \text{K:}\quad 2CH_3C(O)CH_{2_{(a)}} \rightarrow (CH_3)_2CO_{(g)} + C_xH_{y_{(a)}} \quad (6)$$

The reaction of adsorbed $CH_3C(O)CH_{2(a)}$ with small amounts of $HCOOH_{(g)}$, $HDO_{(g)}$, and $H_2O_{(g)}$, introduced during the dosing of $HCOOD_{(g)}$, may also have occurred because the highest purity of HCOOD achieved was only 86 atom % D. Further exchange with a small quantity of background water in the stainless steel dosing lines, despite baking, may also have increased the concentration of these hydrogen-substituted species. Finally, some re-adsorption of $(CH_3)_2CO_{(g)}$, which is pumped very slowly by the ion pump, onto the surface as the crystal cooled to 120 K following the 420 K anneal is possible.

Confirmation of the presence of adsorbed formate following the evolution of acetone-d_1 (*m/q* 59) and acetone-d_0 (*m/q* 58) near 290 K was obtained through the use of EELS. The vibrational spectrum recorded after a surface prepared as described above was exposed to ≈1 langmuir of $HCOOD_{(g)}$ and annealed to 335 K to evolve the acetone products appears in Figure 6. Observed losses are compared with the vibrations of $HCOO_{(a)}$ adsorbed on Ag(110) in Table 3. The majority of the spectrum strongly resembles the EEL spectrum reported for formate adsorbed on Ag(110) in a bidentate configuration following an anneal of formic acid and $O_{(a)}$ to 300 K.[3] The

Table 3. Comparison of Losses Observed Following HCOOD Titration of $CH_3C(O)CH_{2(a)}$ with Vibrational Modes Observed for Formate $HCOO_{(a)}$ on Ag(110)[a]

vibrational mode[b]	335 K anneal	$HCOO_{(a)}$ following 300 K anneal[c]
ν(Ag−O)	280	280 (s)
δ(OCO)	780	780 (m)
π(C−H)	1000	1060 (w)
ν_s(OCO)	1360	1340 (vs)
ν_a(OCO)	1540	1570 (w)
ν(C−H)	2810	2870 (w)
	2960	

[a] All frequencies reported in cm^{-1}. [b] ν = stretch; ν_s = symmetric stretch; ν_a = asymmetric stretch; π = out-of-plane bending; δ = in-plane bending; ϱ_r = rocking; s = strong; m = medium; w = weak; br = broad; v = very; nr = not resolved; n/a = not applicable. [c] From ref 3.

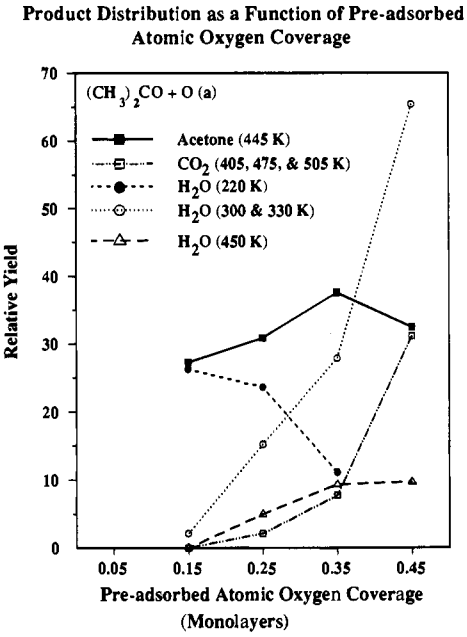

Figure 7. Product distribution for the oxidation of $(CH_3)_2CO$ on Ag(110) as a function of pre-adsorbed atomic oxygen ($O_{(a)}$) coverage.

strong symmetric OCO stretching vibration ν_s(OCO) at 1360 cm^{-1} and less intense asymmetric mode ν_a(OCO) at 1540 cm^{-1} are characteristic of bidentate $HCOO_{(a)}$ at ≥250 K. The losses at 280 cm^{-1} (ν(Ag−O)), 780 cm^{-1} (δ(OCO) of $HCOO_{(a)}$), 1000 cm^{-1} (π(CH)), and 2810/2960 (ν(CH)) are also clearly associated with formate generated during the titration reaction. The small features at 570, 660, 840, 1220, and 1430 cm^{-1} in Figure 6 are attributed to co-adsorbed hydrocarbon fragments produced by the partial oxidation of acetone during the initial anneal.

(d) Product Distribution as a Function of Pre-adsorbed Oxygen Coverage. The distribution of $(CH_3)_2CO_{(g)}$, $H_2O_{(g)}$, and $CO_{2(g)}$ produced as a function of pre-adsorbed atomic oxygen coverage over the range from 0.15 to 0.45 ML of $O_{(a)}$ appears in Figure 7. An acetone exposure of sufficient magnitude to produce adsorbed multilayers (≈3 langmuir) was employed. Contributions to *m/q* 44 and *m/q* 18 due to the fragmentation of acetone at 445 K have been subtracted from the corresponding $CO_{2(g)}$ and $H_2O_{(g)}$ TPRS peak areas. Data for the acetone 330 K state are not included because TPRS peak areas at all atomic oxygen coverages could not be accurately calculated because the 330 K state appears superimposed on the "tail" of the molecular desorption (Figure 1).

Over the range of oxygen coverages studied, the amount of acetone at 445 K increases initially and then remains approximately constant above 0.35 ML of $O_{(a)}$. The amount of

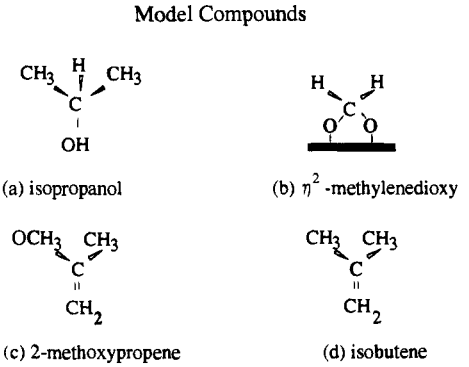

Figure 8. Model compounds whose vibrational spectra were used for reference in the assignment of electron energy loss spectra: (a) 2-propanol (isopropanol), (b) η^2-methylenedioxy, (c) 2-methoxypropene, and (d) isobutene.

$H_2O_{(g)}$ at 220 K decreases substantially with increasing $O_{(a)}$ coverage, however, apparently because the competition between $O_{(a)}$ and $OH_{(a)}$ to react with chemisorbed $(CH_3)_2CO_{(a)}$ to yield $CH_2{=}C(CH_3)O_{(a)}$ and $OH_{(a)}$ or $H_2O_{(a)}$ favors the stronger base, $O_{(a)}$. As a result, the production of $H_2O_{(g)}$ due to $OH_{(a)}$ disproportionation at 300−330 K increases. At $O_{(a)}$ coverages of ≥0.35 ML, $CO_{2(g)}$ evolves at *ca.* 505 K in addition to 405 K and 475 K production in Figure 1 for 0.25 ML of $O_{(a)}$. This increase in $CO_{2(g)}$ production, as well as the evolution of additional $H_2O_{(g)}$ at *ca.* 450 K, reflects additional combustion of acetone fragments due to increased $O_{(a)}$ coverage.

B. Electron Energy Loss Spectroscopy (EELS). The temperature-programmed reaction and surface titration results presented above suggest that both nucleophilic attack at the acyl carbon to yield the reversibly-formed intermediate $(CH_3)_2COO_{(a)}$ and activation of a single C−H bond to produce $CH_3C(O)CH_{2(a)}$ occur during the reaction of acetone with atomic oxygen-activated Ag(110). Through comparison of the vibrational spectra presented below with those reported in the literature for the model compounds 2-propanol (Figure 8a) and η^2-methylenedioxy (Figure 8b), the metallacycle $(CH_3)_2COO_{(a)}$ (**1**)

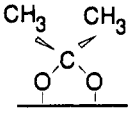

1

has been identified as the intermediate giving rise to $(CH_3)_2CO$ at 215 and 330 K. Similarly, the presence of adsorbed acetone enolate (**2**), bound to Ag(110) via the oxygen atom, has been

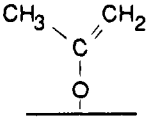

2

confirmed via a comparison of observed loss frequencies with vibrational modes reported for 2-methoxypropene (Figure 8c) and isobutene (Figure 8d). Identification of both intermediates was facilitated by the use of both $(CH_3)_2CO$ and $(CD_3)_2CO$ in EELS experiments in order to differentiate between losses due to skeletal and C−H (C−D) modes.

(a) 110 K. The presence of features in the vibrational spectra of both $(CH_3)_2CO$ and $(CD_3)_2CO$ adsorbed on oxygen-activated Ag(110) (Figures 9a and 10a) which are absent when these compounds are adsorbed on clean Ag(110) (Figures 9b and 10b)

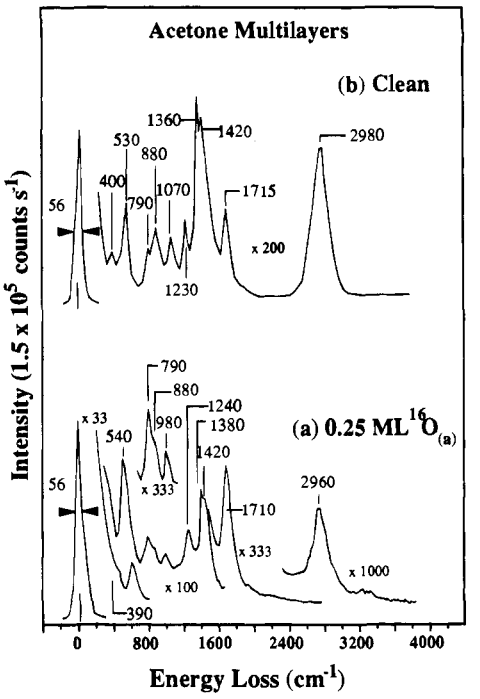

Figure 9. Vibrational spectra recorded following the exposure of Ag(110) activated with 0.25 ML $O_{(a)}$ to multilayers (3 L) of $(CH_3)_2CO_{(g)}$ at 110 K (a) compared with the spectrum obtained following the adsorption of 3 L of acetone on clean Ag(110) (b).

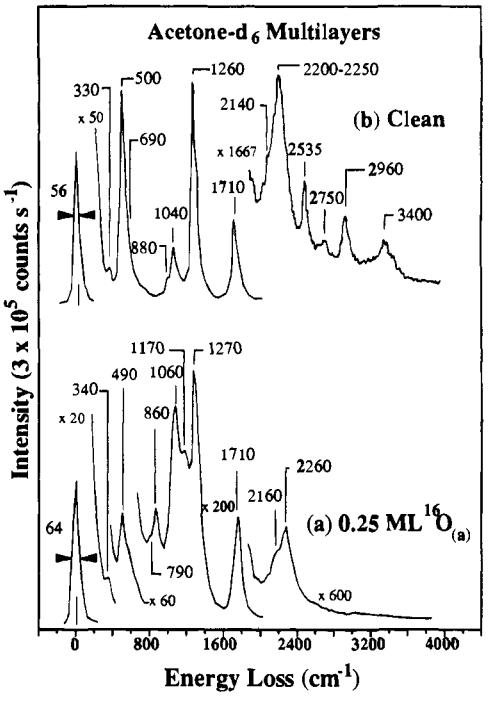

Figure 10. Vibrational spectra recorded following the exposure of Ag(110) activated with 0.25 ML $O_{(a)}$ to multilayers (3 L) of $(CD_3)_2CO_{(g)}$ at 110 K (a) compared with the spectrum obtained following the adsorption of 3 L of acetone-d_6 on clean Ag(110) (b).

suggests that a reaction between $O_{(a)}$ and $(CH_3)_2CO$ ($(CD_3)_2CO$) takes place upon adsorption of the ketone at 110 K. Assignments and a comparison of frequency shifts (ν_H/ν_D) for the two isotopes adsorbed on both the clean and oxygen-activated surfaces appear in Table 4. For the oxygen-activated surface, C−H modes exhibit frequency shifts of 1.26−1.34, whereas skeletal modes show shifts of 0.98−1.15. In both cases, observed frequency shifts are comparable to those exhibited for

Table 4. Comparison of Vibrational Modes Observed for $(CH_3)_2CO$ and $(CD_3)_2CO$ Multilayers Adsorbed on Clean and Oxygen-Activated Ag(110) at 110 K[a]

	$(CH_3)_2CO$			$(CD_3)_2CO$			
mode[b]	$(CH_3)_2CO$ multilayers/ clean Ag(110)	$(CH_3)_2CO_{(a)}$	$(CH_3)_2COO_{(a)}$	$(CD_3)_2CO$ multilayers/ clean Ag(110)	$(CD_3)_2CO_{(a)}$	$(CD_3)_2COO_{(a)}$	ν_H/ν_D
π(C=O)	400	390		330	340		1.15[d]
δ(CO)	530	450		500	490		1.10[e]
$\varrho_r(CH_3)$	880	880	n/a[b,c]	nr	790		
	1070	nr[b]		880	860	860	
ν_s(CC)	790	790		nr	nr		
$\varrho_r(CH_3)^+$	n/a		980[c]	n/a	n/a	n/a	
ν(CCC)			nr			n/a	
ν_s(OCO)	n/a		980[c]	n/a		nr	
ν_a(OCO)	n/a		nr[c]	n/a		1170	
ν_a(CCC)	1230	1240		1270	1270		0.98[e]
$\delta_{s,a}(CH_3)$	1360	1380	1380	1040	1060	1060	1.30[d]
	1420	1420	1420				1.34[d]
ν(C=O)	1715	1710		1710	1710		1.00[e]
$\nu_{s,a}(CH_3)$	nr	2850	2850	2200	2160	2160	1.32[d]
	2980			2250	2260	2260	1.26[d]

[a] All frequencies reported in cm^{-1}. [b] ν = stretch; ν_s = symmetric stretch; ν_a = asymmetric stretch; π = out-of-plane bending; δ = in-plane bending; ϱ_r = rocking; γ = wagging; nr = not resolved; n/a = not applicable. [c] For $(CH_3)_2COO_{(a)}$, absence of $\varrho_r(CH_3)$ is due to coupling of these vibrations with ν(CCC). See text for further discussion. [d] Error = ±0.05. [e] Error = ±0.02.

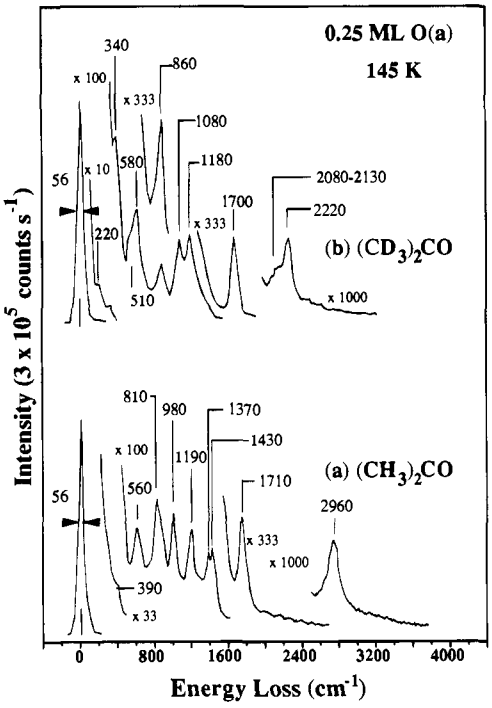

Figure 11. Vibrational spectra recorded following the anneal to 145 K of a Ag(110) surface covered with 0.25 ML of $O_{(a)}$ and exposed to 3 L (multilayers) of (a) $(CH_3)_2CO$ and (b) $(CD_3)_2CO_{(g)}$ at 110 K. The sample was cooled to 110 K prior to recording each spectrum.

$(CH_3)_2CO$ and $(CD_3)_2CO$ adsorbed on clean Ag(110). However, features unlike those in the clean surface spectra appear at 790 and 980 cm^{-1} in the $(CH_3)_2CO$ spectrum and at 790 and 1170 cm^{-1} in the $(CD_3)_2CO$ spectrum on the oxygen-activated surface. By annealing the surface to 145 K to desorb the multilayer, the new features associated with species unique to the oxidized surface are revealed more clearly.

(b) 145 K. Vibrational spectra recorded after annealing the surface to 145 K and subsequently cooling it to 110 K are shown in Figure 11, a ($(CH_3)_2CO$) and b ($(CD_3)_2CO$). Assignments and frequency shifts (ν_H/ν_D) appear in Table 5. Frequency shifts over a range of 1.01−1.15 are observed for skeletal modes, whereas larger shifts of 1.27−1.41 are again seen for C−H losses. Based on a comparison of these shifts with those observed for multilayers adsorbed on clean Ag(110) (Table 4),

Table 5. Vibrational Modes of Adsorbed Intermediates Following 145 K Anneal[a]

	$(CH_3)_2CO$		$(CD_3)_2CO$		
mode[b]	$(CH_3)_2$-$CO_{(a)}$	$(CH_3)_2$-$COO_{(a)}$	$(CD_3)_2$-$CO_{(a)}$	$(CD_3)_2$-$COO_{(a)}$	ν_H/ν_D
π(C=O)	390		340		1.15[d]
δ(C=O)	560		510		1.09[d]
δ(OCO)		nr[b]		580	
ν(CC)	810		nr		
$\varrho_r(CH_3) + \nu$(CCC)		980[c]		n/a[b]	
		1190		n/a	
$\varrho_r(CH_3)$	nr	n/a[b]	800	800	
			860	860	
ν_s(OCO)		980		1080	0.98[d]
ν_a(OCO)		1190[c]		1180	1.01[d]
$\delta_{s,a}(CH_3)$	1370	1370	1080	1080	1.27[e]
	1430	1430			1.32[e]
ν(C=O)	1710		1700		1.01[d]
$\nu_{s,a}(CH_3)$	2960	2960	2080−2130	2080−2130	1.41[e]
			2220		1.33[d]

[a] All frequencies reported in cm^{-1}. [b] ν = stretch; ν_s = symmetric stretch; ν_a = asymmetric stretch; π = out-of-plane bending; δ = in-plane bending; ϱ_r = rocking; γ = wagging; nr = not resolved; n/a = not applicable. [c] For $(CH_3)_2COO_{(a)}$ absence of $\varrho_r(CH_3)$ is due to coupling of these vibrations with ν_a(CCC) to produce modes at 980 cm^{-1} and 1190 cm^{-1}. See text for further discussion. [d] Error = ±0.02. [e] Error = ±0.05.

several losses may be readily assigned. The presence of the ν(C=O) vibration at 1710 cm^{-1}, a value nearly identical with that observed for multilayers adsorbed on clean Ag(110), provides the strongest evidence that acetone molecules remain adsorbed intact. Other skeletal modes which may be readily attributed to acetone include the C=O out-of-plane bending vibration (π(C=O)) at 390 cm^{-1} (340 cm^{-1} for $(CD_3)_2CO$), the C=O in-plane bending vibration (δ(C=O)) at 560 cm^{-1} (510 cm^{-1} for $(CD_3)_2CO$), the C−C stretching mode ν(CC) at 810 cm^{-1} (not resolved for $(CD_3)_2CO$), and the C=O stretching vibration (ν(C=O)) at 1710 cm^{-1} (1700 cm^{-1} for $(CD_3)_2CO$)). Modes associated with methyl groups include the symmetric and asymmetric stretching vibrations ($\nu_{s,a}(CH_3)$) at 2960 cm^{-1} and the symmetric and asymmetric inplane deformations ($\delta_{s,a}(CH_3)$) at 1370 and 1430 cm^{-1}, respectively. The rocking vibration ($\varrho_r(CH_3)$) expected at ≈ 1050 cm^{-1} ($\nu_H/\nu_D \approx 1.22$ from Table 4) is not resolved from the loss at 980 cm^{-1}, the identity of which will be discussed below. Methyl-d_3 (CD_3)

modes present include $\nu_a(CD_3)$ at 2220 cm^{-1}, $\nu_s(CD_3)$ at 2080–2130 cm^{-1}, $\delta_{s,a}(CD_3)$ at 1080 cm^{-1}, and $\gamma(CD_3)$ at 860 cm^{-1}.

Evidence of an adsorbed intermediate different from acetone itself is provided by the losses at 980 and 1190 cm^{-1} in the $(CH_3)_2CO$ spectrum, which we associate with the bidentate intermediate $(CH_3)_2COO_{(a)}$ (**1**). The presence of both of these features in the acetone-d_0 spectrum and the single loss at 1180 cm^{-1} in the acetone-d_6 spectrum suggests that rehybridization of the central carbon from sp^2 to sp^3 has occurred. These features appear to arise from distinct shifts in $\nu_a(CCC)$ and $\varrho_r(CH_3)$ as compared with the spectrum of acetone on clean Ag(110) (Figure 9a). For 2-propanol (Figure 8a), which possesses a central sp^3 carbon, vibrations at 953 cm^{-1} (strong) and 1130 and 1160 cm^{-1} (weak) are observed in the FTIR spectrum due to coupling of the methyl $\varrho_r(CH_3)$ and C–C–C stretching ($\nu_s(CCC)$) modes. No coupling of $\varrho_r(CD_3)$ and $\nu_s(CCC)$ is observed for perdeuterio-2-propanol due to the red shift of the methyl rocking modes to *ca.* 880 cm^{-1} upon deuteration. The shifts observed for the frequencies corresponding to $\nu_a(CCC)$ and $\varrho_r(CH_3)$ for acetone-d_0 are, therefore, consistent with the assignment of the 980 and 1190 cm^{-1} loss features in Figure 9a (110 K) and Figure 11a (145 K) to $\varrho_r(CH_3)$–$\nu(CCC)$ coupling. The presence of a mode at 1180 cm^{-1} in the $(CD_3)_2CO$ spectrum (Figure 11b) suggests that there is also a skeletal contribution to the 1190 cm^{-1} loss in the $(CH_3)_2CO$ spectra. We assign this mode to the asymmetric stretching vibration of the O-C-O bonds ($\nu_a(OCO)$) in $(CH_3)_2COO_{(a)}$ and $(CD_3)_2COO_{(a)}$ by comparison with η^2-methylenedioxy (Figure 8b). In $H_2COO_{(a)}$, derived from the reaction of $H_2CO_{(g)}$ with $O_{(a)}$ on Ag(110), the asymmetric ($\nu_a(OCO)$) stretching mode is reported at 1100 cm^{-1} and the symmetric ($\nu_s(OCO)$ stretching mode at 980 cm^{-1}.[2] Therefore, some contribution to the 980 cm^{-1} loss feature in the $(CH_3)_2CO$ spectrum (Figure 11a) may be due to the $\nu_s(OCO)$ mode as well. This loss feature is not expected to be distinguishable from the strong CD_3 scissoring ($\delta_{s,a}(CD_3)$) modes near 1060 cm^{-1} in the $(CD_3)_2CO$ spectrum.

Finally, the new feature at 580 cm^{-1} in Figure 11b is also attributed to the $(CD_3)_2COO_{(a)}$ intermediate. This loss is assigned to the in-plane bending vibration of the O-C-O bond ($\delta(OCO)$) based on the fact that its intensity relative to that of the $\nu_a(OCO)$ mode remains constant upon annealing the sample to both 190 and 300 K. If this loss were associated with molecularly adsorbed $(CD_3)_2CO$, the intensity of this mode should decrease upon the desorption of the 170 and 215 K acetone states. The 1700 cm^{-1} loss associated with $\nu(C{=}O)$ of molecularly adsorbed $(CD_3)_2CO$, for example, decreases in intensity upon annealing the surface to 190 K and disappears by 300 K. We also note that for $H_2COO_{(a)}$ adsorbed on Ag(110), $\delta(OCO)$ is observed at 620 cm^{-1}.[2]

(c) 190 K. After the surface is annealed to 190 K to further desorb acetone from the 170 K molecular acetone state and cooled to 110 K, the intensity of the C=O stretching vibration $\nu(C{=}O)$ decreases substantially (Figure 12b), a result consistent with the desorption of molecular acetone. In addition, this mode shifts from 1710 cm^{-1} (Figure 12a) to 1680 cm^{-1} (Figure 12b) because of a slight weakening of the carbonyl bond due to a change in coordination to the Ag(110) surface. The 980 and 1160 cm^{-1} loss features attributed to a combination of $\varrho_r(CH_3)$–$\nu(CCC)$ coupling and $\nu_{s,a}(OCO)$ stretching vibrations in $(CH_3)_2COO_{(a)}$ and $(CD_3)_2COO_{(a)}$ persist following the 190 K anneal. The remaining loss features closely resemble the 145 K acetone-d_0 spectrum with which the 190 K spectrum is compared in Figure 12.

(d) 300 K. After the surface is annealed to 300 K, evidence

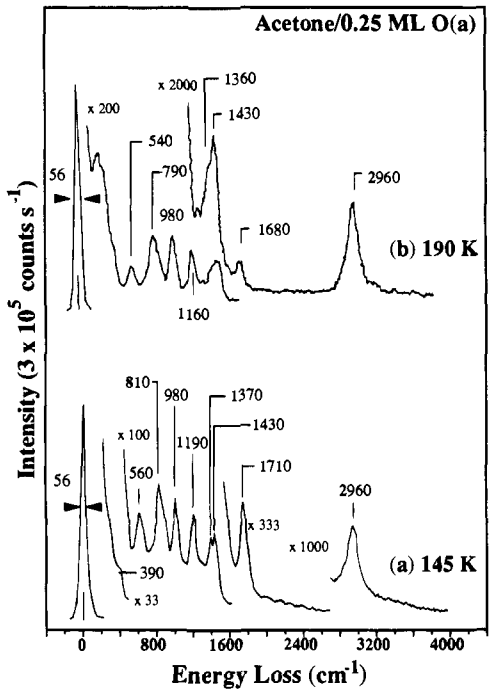

Figure 12. Vibrational spectra recorded following the anneal to (a) 145 K and (b) 190 K of a Ag(110) surface activated with 0.25 ML of $O_{(a)}$ and exposed to 3 L (multilayers) of $(CH_3)_2CO$ at 110 K. The sample was cooled to 110 K prior to recording each spectrum.

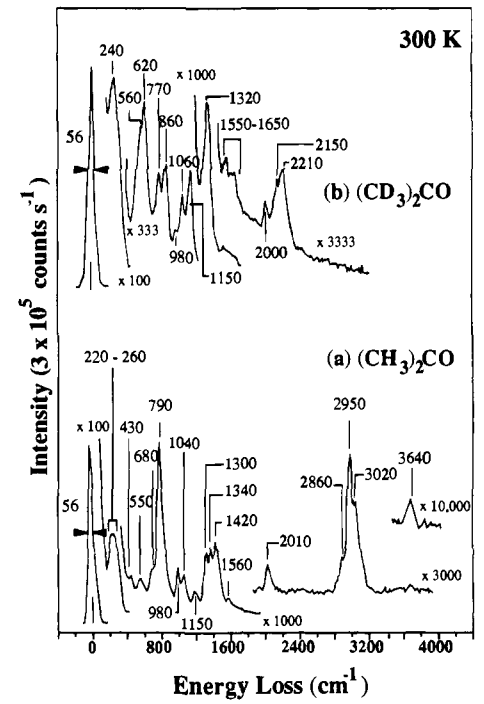

Figure 13. Vibrational spectra recorded following the anneal to 300 K of a Ag(110) surface activated with 0.25 ML of $O_{(a)}$ and exposed to 3 L (multilayers) of (a) $(CH_3)_2CO$ and (b) $(CD_3)_2CO_{(g)}$ at 110 K. The sample was cooled to 110 K before recording each spectrum.

for the presence of co-adsorbed $CH_2{=}C(CH_3)O_{(a)}$, $(CH_3)_2COO_{(a)}$, $OH_{(a)}$, and $CO_{(a)}$ is obtained (Figure 13 and Table 6). During this anneal, the evolution of both acetone at 215 K and $H_2O_{(g)}$ at 220 K occurs, as well as the onset of $OH_{(a)}$ disproportionation to yield $H_2O_{(g)}$ and $O_{(a)}$. No acetone remains adsorbed: the intense loss features over 1700 cm^{-1} associated with the carbonyl stretching vibration have disappeared. The weaker losses near 390 (for acetone-d_0) and 340 cm^{-1} (acetone-

Table 6. Vibrational Modes of Adsorbed Intermediates Following 300 K Anneal[a]

mode[b]	$CH_3C-(CH_2)O_{(a)}$	$(CH_3)_2-COO_{(a)}$	$CD_3C-(CD_2)O_{(a)}$	$(CD_3)_2-COO_{(a)}$	ν_H/ν_D
δ(CCC)	430[c]		nr		
δ(CO)		550		560	0.98[e]
τ(=CH_2)	680		nr[b]		
γ(=CH_2)	790		620		1.27[e]
ϱ_r(=CH_2)	980		770		1.27[e]
$\varrho_r(CH_3) + \nu$(CCC)		980[d]		n/a	
		1150		n/a	
ν_s(OCO)		980[d]		980	1.00[e]
$\varrho_r(CH_3)$	1040	n/a[d]	860	860	1.21[e]
ν_a(OCO)		1150[d]		1150	1.00[e]
ν_a(C−O)	1300		1320		0.98[e]
$\delta_{s,a}(CH_3)$	1340	1340	1060	1060	1.26[f]
	1420	1420			1.34[f]
ν(C=C)	1560[g]		1550−1650[d]		0.97[f]
$\nu_{s,a}(CH_3)$	2860	2860	2150	2150	1.33[e]
	2950	2950	2210	2210	1.33[e]
ν(=CH_2)	3020	n/a	nr	n/a	
additional losses:					
ν(C≡O) of $CO_{(a)}$	2010		2000		
ν(O−H) of $OH_{(a)}$	3640		nr		

[a] All frequencies reported in cm^{-1}. [b] ν = stretch; ν_s = symmetric stretch; ν_a = asymmetric stretch; π = out-of-plane bending; δ = in-plane bending; ϱ_r = rocking; τ = twisting; γ = wagging; nr = not resolved; n/a = not applicable. [c] Tentative assignment. [d] For $(CH_3)_2COO_{(a)}$, absence of $\varrho_r(CH_3)$ losses is due to coupling of these vibrations with ν(CCC) to produce modes at 980 and 1150 cm^{-1}. See text for further explanation. [e] Error = ±0.02. [f] Error = ±0.05. [g] Tentative assignment; these losses could also be due to overtones of 780 cm^{-1} (γ(=CH_2)) and 770 cm^{-1} (ϱ_r(=CD_2)) modes, respectively.

d_6) due to the out-of-plane bending (π(C=O)) vibrations have also vanished.

The chief indication of $(CH_3)_2COO_{(a)}$ following the 300 K anneal is the persistence of the ν_s(OCO) and ν_a(OCO) modes at 980 and 1150 cm^{-1}, respectively, for both acetone-d_0 (Figure 13(a)) and acetone-d_6 (Figure 13b). The frequency shift (ν_H/ν_D) ratio of 1.0 for both modes confirms that they are skeletal in origin. The reduced intensity of these losses relative to the height of the elastic peak arises from the evolution at 215 K of acetone produced by C−O bond scission in $(CH_3)_2COO_{(a)}$. The greater intensity of the 980 cm^{-1} loss in the $(CH_3)_2CO$ spectrum is attributed to contributions from both $\varrho_r(CH_3)-\nu$(CCC) coupling of $(CH_3)_2COO_{(a)}$ and ϱ_r(=CH_2) of co-adsorbed CH_2=$C(CH_3)O_{(a)}$ (discussed below). The loss at 550 cm^{-1} (560 cm^{-1} for $(CD_3)_2COO_{(a)}$) previously assigned to δ(CO) is also evident.

The intense mode at 790 cm^{-1} (γ(=CH_2)), the weak feature at 680 cm^{-1} (τ(=CH_2)), the shoulder at 3020 cm^{-1} (ν(=CH_2) or $\nu_a(CH_3)$), and the weak loss at 3600 cm^{-1} (ν(OH)) in Figure 13a are indicative of C−H bond scission to form the enolate CH_2=$C(CH_3)O_{(a)}$ and hydroxyl groups $OH_{(a)}$. The γ(=CD_2) loss appears at 620 cm^{-1} ($\nu_H/\nu_D \approx 1.27$) in the acetone-d_6 spectrum (Figure 13b), but the corresponding τ(=CD_2), ν(OD), and ν_a(=CD_2) ($\nu_a(CD_3)$) features were not resolved. The presence of modes associated with the =CH_2 (=CD_2) moiety suggests that the enolate bonds to the surface via a Ag-O bond as in **2**. Note that **2** is not intended to accurately represent the orientation of the enolate with respect to the Ag(110) surface. The ν(OH) stretching vibration at 3600 cm^{-1} stems from hydroxyl groups generated by C−H bond scission, and the intensity of this mode is weak because $H_2O_{(g)}$ evolution due to hydroxyl disproportionation has begun by this temperature. The 790 cm^{-1} loss is now the strongest mode in the spectrum and is primarily attributed to the wagging vibration (γ(=CH_2)) of the terminal =CH_2 group, generally one of the strongest bands in the vibrational spectra of olefins, rather than to ν_s(CCC).[19,20] The shift of this mode to 798 cm^{-1} in the spectrum of the model compound 2-methoxypropene ($CH_3C(OCH_3)$=CH_2, isopropenyl methyl ether) (Figure 8c) from the characteristic frequency of 890 cm^{-1} for the wagging vibration of a hydrocarbon vinylidene (R_2C=CH_2) has been explained by electron donation from oxygen to the terminal double bond, which causes it to weaken: CH_3-O-$C(CH_3)$=CH_2 ↔ CH_3-O^+=$C(CH_3)CH_2^-$.[21,22] The assignment of γ(=CH_2) to the mode observed at 790 cm^{-1} is, therefore, reasonable.

Additional evidence that CH_2=$C(CH_3)O_{(a)}$ (**2**) is adsorbed on Ag(110) with the carbon−carbon double bond (C=C) intact is provided by the reproducible loss at 3020 cm^{-1}. This frequency lies between the symmetric and asymmetric C−H stretching frequencies reported for the terminal double bond ($\nu_{s,a}$-(=CH_2)) (3131 and 2984 cm^{-1}) and near the higher of the frequencies observed for the doubly degenerate asymmetric methyl stretching vibration ($\nu_a(CH_3)$) (3026 and 2971 cm^{-1}) in the Raman spectrum of 2-methoxypropene (Figure 8c).[21] This mode is not present in acetone. Furthermore, no feature near 3020 cm^{-1} was apparent when $(CH_3)_2CO_{(a)}$ and $(CH_3)_2COO_{(a)}$ were co-adsorbed at 145 and 190 K. Therefore, the loss at 3020 cm^{-1} is assigned to ν(=CH_2) or $\nu(CH_3)$ of CH_2=$C(CH_3)O_{(a)}$. The weak losses at 1560 cm^{-1} (acetone-d_0) and 1550 cm^{-1} (-d_6) are tentatively assigned to the stretching vibration (ν(C=C)) of the asymmetrically substituted carbon−carbon double bond of acetone enolate because these weak vibrations could be associated with first overtones of the 790 cm^{-1} (γ(=CH_2)) and 770 cm^{-1} (ϱ_r(=CD_2)) modes. The modes at 1300 (acetone-d_0) and 1320 cm^{-1} (-d_6) are attributed to the presence of the C−O single bond stretch of the enolate, an assignment supported by their continued presence following an anneal of the surface to 360 K (see below) and the fact that the asymmetric C−O stretching vibration (ν_a(CO)) of 2-methoxypropene ($CH_3C(OCH_3)$=CH_2) appears at 1294 cm^{-1} in the gas-phase Raman spectrum of that compound.[22] Finally, the new feature at 430 cm^{-1} is tentatively assigned to the skeletal deformation of the enolate carbon skeleton (δ(CCC)), also by comparison with the gas-phase Raman spectrum of 2-methoxypropene, in which this mode gives rise to a band at 413 cm^{-1}.

Vibrational modes associated with two additional adsorbates may be readily identified as well. Present at 2010 cm^{-1} in the $(CH_3)_2CO$ spectrum and at 2000 cm^{-1} in the $(CD_3)_2CO$ spectrum are losses associated with the stretching vibration (ν(C≡O)) of carbon monoxide. At 3640 cm^{-1} in the acetone-d_0 spectrum, the sharp loss associated with adsorbed hydroxyl $OH_{(a)}$ groups appears; however, the corresponding mode was not observed for acetone-d_6.

The presence of adsorbed CO on Ag(110) at 300 K indicates that this species, presumably generated on the surface due to the combustion of acetone by atomic oxygen, is stabilized by the presence of co-adsorbates. This loss disappears following an anneal of the surface to 419 K, during which $CO_{2(g)}$ evolves (at 405 K). Furthermore, there is no evidence of $CO_{(a)}$ at lower annealing temperatures as would be expected if the adsorption of carbon monoxide occurred owing to an elevated level of CO in the UHV chamber background gas. Since no carbon monoxide evolves into the gas phase in the acetone TPRS experiments, $CO_{(a)}$ formed must be scavenged by oxygen atoms released by (a) hydroxyl disproportionation (eq (7)) and (b)

(19) Sheppard, N.; Simpson, D. M. *Q. Rev. Chem. Soc.* **1952**, *6*, 1.
(20) Hess, B.; Bruna, P. J.; Buenker, R. J.; Peyerimhoff, S. D. *Chem. Phys.* **1976**, *18*, 267.
(21) Gallinella, E.; Pincelli, U.; Cadioli, B. *J. Mol. Struct.* **1983**, *99*, 31.
(22) Potts, W. J.; Nyquist, R. A. *Spectrochim. Acta* **1959**, *15*, 679.

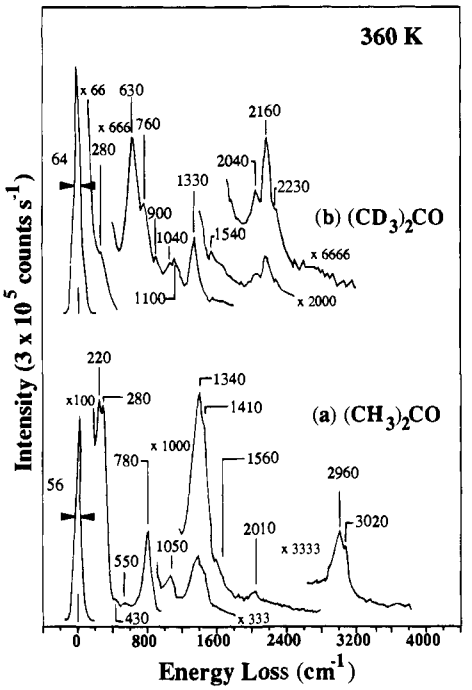

Figure 14. Vibrational spectra recorded following the anneal to 360 K of a Ag(110) surface covered with 0.25 ML of $O_{(a)}$ and exposed to 3 L (multilayers) of (a) $(CH_3)_2CO$ and (b) $(CD_3)_2CO_{(g)}$ at 110 K. The sample was cooled to 110 K before recording each spectrum.

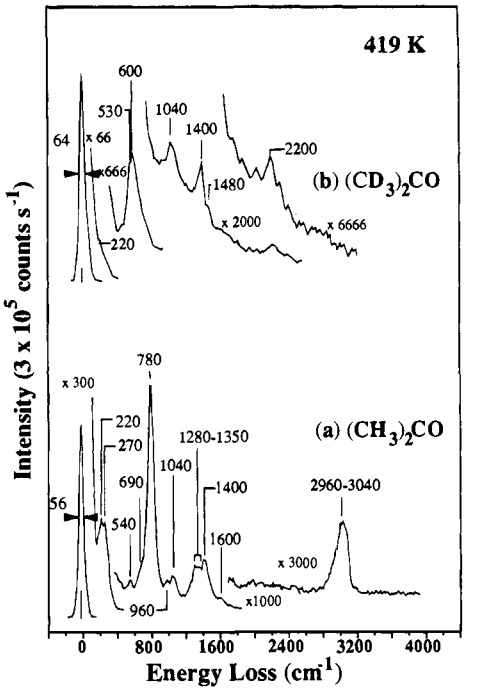

Figure 15. Vibrational spectra recorded following the anneal to 419 K of a Ag(110) surface covered with 0.25 ML of $O_{(a)}$ and exposed to 3 L (multilayers) of (a) $(CH_3)_2CO$ and (b) $(CD_3)_2CO_{(g)}$ at 110 K. The sample was cooled to 110 K prior to recording each spectrum.

Table 7. Vibrational Modes of Adsorbed Intermediates Following 360 K Anneal[a]

vibrational mode[b]	$CH_2{=}C(CH_3)O_{(a)}$	$CD_2{=}C(CD_3)O_{(a)}$	$CO_{(a)}$	ν_H/ν_D[d]
ν(Ag−O)	220	280		
	280			
δ(CCC)	430	nr[b]		
δ(CO)	550	nr		
γ(=CH_2)	780	630		1.23
ν_s(C−O)	780	760		1.03
ϱ_r(=CH_2)	980	760		1.29
ϱ_r(CH_3)	1050	900		1.17
$\delta_{s,a}$(CH_3)	1340	1040		1.29
	1410	1100		1.28
ν_a(C−O)	1340	1330		1.01
ν(C=C)	1560[c]	1540		1.01
ν(C≡O)			2010	
$\nu_{s,a}$(CH_3)	2960	2040		
		2160		
		2230		
ν(=CH_2)	3020	nr		

[a] All frequencies reported in cm^{-1}. [b] ν = stretch; ν_s = symmetric stretch; ν_a = asymmetric stretch; π = out-of-plane bending; δ = in-plane bending; ϱ_r = rocking; γ = wagging; nr = not resolved. [c] Tentative assignment; these losses could also be due to first overtones of 780 cm^{-1} (γ(=CH_2)) and 760 cm^{-1} (ϱ_r(=CD_2)), respectively. [d] Error = ±0.05.

C−O bond cleavage to produce acetone and $O_{(a)}$ (eq (8)). Carbon dioxide $CO_{2(g)}$ subsequently evolves at 405 K (eq (9)).

$$300\text{–}330\ \text{K}: \quad 2OH_{(a)} \rightarrow H_2O_{(g)} + O_{(a)} \tag{7}$$

$$330\ \text{K}: \quad (CH_2)_2COO_{(a)} \rightarrow (CH_3)_2CO_{(g)} + O_{(a)} \tag{8}$$

$$405\ \text{K}: \quad CO_{(a)} + O_{(a)} \rightarrow CO_{2(g)} \tag{9}$$

(e) 360 K. After an anneal of the Ag(110) surface to 360 K, during which $H_2O_{(g)}$ and $(CH_3)_2CO_{(g)}$ evolve at 300−330 K and 330 K, respectively, and subsequent cooling to 110 K, the losses associated with the bidentate intermediate $(CH_3)_2COO_{(a)}$ (**1**) have disappeared (Figure 14, a and b); Table 7). This species, therefore, must give rise to the 330 K acetone state. Acetone enolate (**2**), carbon monoxide, and hydrocarbon fragments remain co-adsorbed. All of the modes assigned to these species in the 300 K spectra (Figure 13) are still evident with the exception of the weak 680 cm^{-1} loss assigned to τ(=CH_2) at 300 K. As above, the weak feature which appears at 430 cm^{-1} in the spectrum of $CH_2{=}C(CH_3)O_{(a)}$ is tentatively assigned to the δ(CCC) skeletal deformation by comparison with the Raman spectrum of 2-methoxypropene (Figure 8c).[21]

The absence of both ν(C=O) at ≈1700 cm^{-1} and π(C=O) at ≈390 cm^{-1} following the 360 K anneal provides additional evidence that acetone enolate is adsorbed on Ag(110) via the oxygen atom, not the terminal carbon. If the enolate were adsorbed via a Ag−C bond, then the carbonyl stretching vibration ν(C=O) would be observed unless the C=O bond was oriented parallel to the surface. In this configuration the out-of-plane π(C=O) mode would be expected to appear at *ca.* 390 cm^{-1} in a vibrational spectrum recorded in the specular direction.

The possibility that co-adsorbed carbonate $CO_{3(a)}$ is the intermediate giving rise to $CO_{2(g)}$ at *ca.* 405 K can be ruled out by the absence of the out-of-plane bending $\pi(CO_3)$ mode expected for this species at 850 cm^{-1}.[23] If the losses at 1050 and 1360 cm^{-1} in Figure 14a and at 1040 and 1400 cm^{-1} in Figure 14b were due to the C−O bond stretch (ν(CO)) and symmetric O=C=O bond stretch (ν_s(O=C=O)) of $CO_{3(a)}$, then the 850 cm^{-1} loss, which is more intense than ν(CO) or ν_s(O=C=O), should also be observed.

(f) 419 K. The spectra obtained following the 419 K anneal (Figure 15, a and b) clearly reveal the vibrational modes associated with acetone enolate (**2**). These losses and their assignments are listed in and compared with the vibrational spectrum of 2-methoxypropene in Table 8.[21] The mode associated with ν(C≡O) has disappeared due to the evolution of $CO_{2(g)}$ at 405 K.

(23) Stuve, E. M.; Madix, R. J.; Sexton, B. *Chem. Phys. Lett.* **1982**, *89*, 48.

Table 8. Comparison of Fundamental Vibrations of 2-Methoxypropene[a,b] and Observed Vibrational Losses for Adsorbed Acetone Enolate Following 419 K Anneal

vibrational mode[c]	2-methoxypropene $CH_3C(OCH_3)=CH_2$	acetone enolate $CH_2=C(CH_3)O_{(a)}$	acetone enolate-d_5 $CD_2=C(CD_3)O_{(a)}$	ν_H/ν_D[h,i]
ν(Ag−O)	n/a[c]	220−270	220	
δ(CCC)	413 (w)	nr[c]	nr	
(C=CH_2) def	510 (mw)	nr	nr	
δ(CCO)	538 (m)	540	nr	
τ(=CH_2)	720 (w)[d]	690	530	1.30
γ(=CH_2)	798 (s)[g]	780	600	1.30
ν_s(CO)	824 (s)	780	750	1.04
ϱ_r(=CH_2)	996 (m)	960[e]	750	1.28
ϱ_r(CH_3)	1045 (w)[d]	1040	750	1.38
	1097 (s)[g]			
ν_a(CO)	1294 (vs)[g]	1280−1350	nr	
	938 (m)[g]			
δ_s(CH_3)	1374 (m)	1280−1350	1040	1.30
δ(=CH_2)	1399 (ms)	1400	1040	1.34
δ_a(CH_3)	1434 (w)	1400	1040	1.34
	1458 (m)[g]			
ν(C=C)	1666 (vs)	1600[f]	1640	0.98
ν_s(CH_3)	2940 (vs)			
ν_s(=CH_2)	2984 (w)			
ν_a(CH_3)	2971 (m)[g]	2960−3040	2200	1.34−1.38
	3026 (m)			
ν_a(=CH_2)	3131 (m)			

[a] From ref 21. Vibrations associated with the methoxy (OCH_3) group are not listed. [b] Gas-phase Raman frequencies, unless otherwise noted. [c] All frequencies reported in cm^{-1}; ν = stretch; ν_s = symmetric stretch; ν_a = asymmetric stretch; π = out-of-plane bending; δ = in-plane bending; ϱ_r = rocking; γ = wagging; τ = twisting; def. = deformation; nr = not resolved; n/a = not applicable. [d] Liquid-phase Raman frequency. [e] Tentative assignment; could also be ν_a(CO). [f] Tentative assignment; may also be first overtone of 780 cm^{-1} (γ(=CH_2)). [g] Gas-phase infrared frequency. [h] For comparison with ν_H/ν_D for similar modes in isobutylene (isobutylene-d_8), see text. 2-methoxypropene-d_8 spectrum not available. [i] Error = ±0.05.

In Figure 15a the major features associated with the terminal double bond of acetone enolate are observed: γ(=CH_2) at 780 cm^{-1} and τ(=CH_2) at 690 cm^{-1}. The corresponding features in the Raman spectrum of 2-methoxypropene are found at 798 and 720 cm^{-1} (Table 8).[21] The corresponding modes for acetone enolate-d_5 appear at 600 cm^{-1} (γ(=CD_2)) and 530 cm^{-1} τ(=CD_2), respectively, in Figure 15b. Because the vibrational spectrum of 2-methoxypropene-d_8 ($CD_3C(OCD_3)=CD_2$) was not available, ν_H/ν_D ratios for the C−H (C−D) modes of isobutene $(CH_3)_2C=CH_{2(g)}$ and isobutene-d_8 ($(CD_3)_2C=CD_{2(g)}$) were compared with those for adsorbed acetone enolate (acetone enolate-d_5).[24] For example, ν_H/ν_D for the alkene wagging and twisting modes is 1.26 for acetone enolate and 1.30 for the isobutene isotopes (Table 8). The losses at 2960−3040 cm^{-1} in Figure 15a, which appear as a single broad feature as in the 360 K spectrum, are due to the alkene and methyl stretching vibrations ν(=CH_2) and $\nu_{s,a}$(CH_3). The feature at 1040 cm^{-1} is assigned to the CH_3 rocking mode (ϱ_r(CH_3)), a doubly degenerate vibration in 2-methoxypropene which gives rise to Raman bands at 1045 and 1097 cm^{-1}.[21] The =CH_2 rocking mode (ϱ_r(=CH_2)) appears at 960 cm^{-1}. The CD_3 and =CD_2 rocking vibrations appear as a single loss feature at 750 cm^{-1} in the $CD_2=C(CD_3)O_{(a)}$ spectrum (Figure 15a) (ν_H/ν_D = 1.38 for ϱ_r(CH_3) and 1.28 for ϱ_r(=CH_2); for isobutene (isobutene-d_8), 1.17−1.31 and 1.27, respectively). The mode at 1400 cm^{-1} in Figure 15a may be due to either the vinylidene or asymmetric methyl bending vibration (δ(=CH_2) or δ_a(CH_3)). The former mode gives rise to bands at 1458 and 1434 cm^{-1} and the latter to a feature at 1399 cm^{-1} in the Raman spectrum of 2-methoxypropene. The symmetric methyl bending (δ_s(CH_3)) vibration is clearly resolved at 1350 cm^{-1} in Figure 15a. However, in Figure 15b these bending modes (δ_a(CD_3), δ_s(CD_3), and δ(=CD_2)) appear as a single loss at 1040 cm^{-1}.

Assignment of the C−O stretching vibration of acetone enolate may also be made by comparison with the Raman spectrum of 2-methoxypropene; in the spectrum of the latter compound, asymmetric stretching modes ν_a(CO) appear at 1294 and 938 cm^{-1} and symmetric stretching vibrations ν_s(CO) as a single band at 824 cm^{-1}.[21] The loss at 1280 cm^{-1} in Figure 15a is, therefore, assigned to the asymmetric stretching vibration ν_a(C−O). The corresponding modes is obscured in the $CD_2=C(CD_3)O_{(a)}$ spectrum (Figure 15b). The features expected at *ca.* 938 and 824 cm^{-1} for $CH_2=C(CH_3)O_{(a)}$ are not resolved from the rocking ϱ_r(=CH_2) and wagging γ(=CH_2) vibrations at 960 and 780 cm^{-1}, respectively. The mode at 540 cm^{-1} in Figure 15a is assigned to the skeletal bending mode δ(CCO), also by comparison with the Raman spectrum of 2-methoxypropene in which this vibration appears at 538 cm^{-1}. In the spectrum of acetone enolate-d_5 (Figure 15b), this vibration is not resolved from the strong twisting τ(=CD_2) mode at 530 cm^{-1}. Finally, the loss at 1600 cm^{-1} in the $CH_2=C(CH_3)O_{(a)}$ spectrum is tentatively assigned to the C=C stretching mode ν(C=C); however, this feature might due to the first overtone of the wagging mode γ(=CH_2). The loss features at 1400 and 1480 cm^{-1} in Figure 15b may include overtones or combination bands as well. Finally, the loss at 220−270 cm^{-1} in Figure 15, a and b, is due to the metal−oxygen stretching vibration (ν(Ag−O)) of the enolate.

C. Discussion. The stabilization of compounds containing electron-deficient sites by atomic oxygen and subsequent oxidation of these compounds by $O_{(a)}$ are mechanisms characteristic of the behavior of atomic oxygen on Ag(110). Similarly, oxidation via scission of acidic C−H bonds is a hallmark reaction. Atomic oxygen reacts with acetone, a compound which contains both an electron-deficient carbonyl carbon and two equivalent methyl groups with acidic C−H bonds, via both mechanisms.

The reaction of acetone with 0.25 ML of atomic oxygen on Ag(110) upon adsorption of the ketone at 110 K is clearly indicated by vibrational spectra which show that molecular $(CH_3)_2CO_{(a)}$ and the metallacycle $(CH_3)_2COO_{(a)}$ are co-adsorbed (Figure 9b and 10b). Reversible formation of $(CH_3)_2COO_{(a)}$ (**1**) is also suggested by the results of isotopic labeling

(24) Pathak, C. M.; Fletcher, W. H. *J. Mol. Spectrosc.* **1969**, *31*, 32.

experiments in which reversible exchange between surface $^{18}O_{(a)}$ and oxygen in $(CH_3)_2C^{16}O_{(a)}$ occurs to yield approximately equal quantities of $(CH_3)_2C^{16}O_{(g)}$ and $(CH_3)_2C^{18}O_{(g)}$ at both 215 and 330 K. Furthermore, vibrational spectra obtained following anneals of the surface to 190 and 300 K confirm the continued presence of $(CH_3)_2COO_{(a)}$, among other species. Since $(CH_3)_2C^{18}OO_{(a)}$ gives rise to $(CH_3)_2C^{18}O_{(g)}$ and $(CH_3)_2C^{16}O_{(g)}$ at 330 K as well as 215 K, it seems likely that this metallacycle is either stabilized to the higher temperature by the presence of co-adsorbates or is adsorbed at defect sites.

Confirmation of the scission of a single C−H bond in acetone to form acetone enolate (**2**) at a low temperature is provided by the production of $H_2O_{(a)}$ at 220 K in TPRS and the evolution of $CH_3C(O)CH_2D$ (*m/q* 59) as the only deuterated product in surface titration experiments. Furthermore, vibrational spectra obtained following an anneal of the surface to 300 K to desorb molecular acetone and $H_2O_{(g)}$ indicate that a mixture of $CH_2{=}C(CH_3)O_{(a)}$, $(CH_3)_2COO_{(a)}$, $CO_{(a)}$, $OH_{(a)}$, and hydrocarbon fragments are co-adsorbed. The subsequent evolution of acetone at 445 K is attributed to the disproportionation of $CH_2{=}C(CH_3)O_{(a)}$. Whereas vibrational data indicate that acetone enolate remains adsorbed following an anneal of the surface to 419 K, detailed comparisons of the fragmentation pattern of the 445 K product state with both an experimentally-determined fragmentation pattern for acetone (70 eV ionization energy) and a published report of the fragmentation pattern for acetone enol (75 eV ionization energy) yielded no evidence of an acetone enol product.[12] Note that the disproportionation of acetone enolate to yield $(CH_3)_2CO_{(g)}$ may not be an elementary reaction step. While it could be imagined that the enolate might be formed by "interception" of the enol form due to the existence of a keto−enol equilibrium on the metal surface and subsequent activation of the O−H bond of a surface-bound enol, this pathway seems unlikely. Not only does equilibrium lie heavily on the side of the keto form of acetone, but also $(CH_3)_2CO_{(g)}$ evolves prior to $OH_{(a)}$ formation, a result clearly indicated by both TPRS and vibrational data.

The presence of $CO_{(a)}$ in the vibrational spectra recorded following the 300 K anneal indicates that C−C bond scission also occurs by this temperature. However, no carbon monoxide was detected in the gas phase; $CO_{(a)}$ reacts upon heating with $O_{(a)}$ ($^{18}O_{(a)}$) released during $OH_{(a)}$ disproportionation at 300−330 K to produce an isotopic mixture of $CO_{2(g)}$, $C^{18}OO_{(g)}$, and $C^{18}O_{2(g)}$ at 405 K. The partial oxidation of $(CH_3)_2CO_{(a)}$ to produce $CO_{(a)}$ and adsorbed hydrocarbon fragments is not considered to be an elementary reaction step. Subsequent oxidation of hydrocarbon fragments due to atomic oxygen scavenging yields a mixture of $CO_{2(g)}$ and $H_2O_{(g)}$ isotopes at 450 and 475 K, and for higher $O_{(a)}$ coverages, additional $CO_{2(g)}$ at 505 K. A summary of the proposed reaction steps appears in Figure 16.

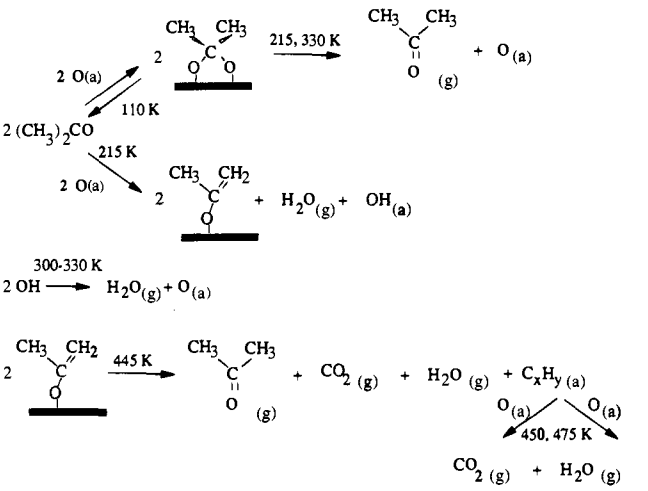

Figure 16. Summary of the proposed mechanism for the reaction of acetone with $O_{(a)}$ on Ag(110).

Thus, the reaction of $O_{(a)}$ with acetone via both nucleophilic attack and an acid−base mechanism confirms that these two mechanisms are competitive reaction pathways on oxygen-activated Ag(110). Furthermore, the facile exchange of oxygen atoms between $(CH_3)_2COO_{(a)}$ and $^{18}O_{(a)}$ in isotope labeling experiments shows that reversible exchange between bidentate intermediates adsorbed on Ag(110) through two oxygen atoms and co-adsorbed oxygen is a general type of reaction on this surface.

Acknowledgment. The authors gratefully acknowledge support of the National Science Foundation (NSF CTS 9005135-A2).

JA941545U